

# Mineral X, a new thalcosite homologue from the Ilímaussaq complex, South Greenland

Contribution to the mineralogy of Ilímaussaq, no. 144

S. KARUP-MØLLER & E. MAKOVICKY



Karup-Møller, S. & Makovicky, E. 2011. Mineral X, a new thalcosite homologue from the Ilímaussaq complex, South Greenland © 2011 by Bulletin of the Geological Society of Denmark, Vol. 59, pp. 13–22. ISSN 0011–6297. (www.2dgf.dk/publikationer/bulletin) <https://doi.org/10.37570/bgsd-2011-59-02>

Mineral X is assumed to be a new member of the thalcosite homologous series with the structural formula  $\text{TlCu}_{2N}\text{S}_{2N+1}$  with  $N=1.5$ . It was found in loose ussingite-analcime boulders on the Taseq slope towards the Narsaq Elv in the northern part of the Ilímaussaq complex in South Greenland in association with chalthallite, cuprostibite, galena, sphalerite, bornite, antimonian silver and seinä-jokite. Supergene alteration has resulted in a number of secondary Cu-Sb-minerals. The primary ore minerals appear to have crystallized contemporaneously under low S-fugacities.

Received 8 April 2010  
Accepted in revised form  
15 December 2010  
Published online  
11 March 2011

**Keywords:** Tl-minerals, thalcosite homologous series, low S-fugacities, chalthallite, cuprostibite, ussingite veins, South Greenland, Ilímaussaq, Taseq.

*Sven Karup-Møller (svka@byg.dtu.dk) Department of Civil Engineering, Technical University of Denmark; Emil Makovicky (Emilm@geo.ku.dk), Institute of Geography and Geology, University of Copenhagen, Denmark.*

At present three primary thallium bearing minerals have been discovered at the Ilímaussaq complex in South Greenland: chalthallite, rohaite and thalcosite (Semenov *et al.* 1967; Karup-Møller 1978a; Kovalenker *et al.* 1978; Makovicky *et al.* 1980; Karup-Møller and Makovicky 2001). All minerals referred to in this paper are listed in Table 1. Chalthallite and rohaite are known only from their type localities within the Ilímaussaq complex. Chalthallite occurs in ussingite veins in naujaite on the Taseq slope towards Narsaq Elv in the northern part of the complex. Associated ore minerals are cuprostibite, native silver, chalcocite, gudmundite and thalcosite. Rohaite was found in an analcime-sodalite vein in lujavrite at Kvanefjeld. Associated primary ore minerals here are cuprostibite, chalcocite, sphalerite, loellingite and antimonian silver. Rohaite is partly altered to secondary digenite-senarmontite aggregates. The thalcosite type locality is Talnakh in the Norilsk region, Siberia, Russia (Kovalenker *et al.* 1978). The mineral has also been found at the Murun massif, Aldan Shield, Yakutia, Russia (Dobrovol'skaya *et al.* 1984); Dobrovol'skaya & Nekrasov 1994), at Rajapura-Dariba, Rajasthan, India (Mookherjee *et al.* 1984) and at Mont Saint-Hilaire, Quebec, Canada (Mandarino & Anderson 1989). Within the Ilímaussaq massif thalcosite has

been found at three localities: at Taseq associated with chalthallite, as minor inclusions in naujaite at the head of Kangerluarsuk fjord in the southern part of the complex and in coarse ussingite associated with cuprostibite at Nakkaalaaq mountain in the north-eastern part of the complex.

## Mineral locations and sample material

In 2006 Tom Weidner found additional chalthallite in two erratic ussingite-analcime boulders some 200 m. apart on the Taseq slope towards the Narsaq Elv. The total amount of material collected was about 5 kg. We assume that these boulders come from the same mineral vein system that hosts the chalthallite type material. They are referred to as boulder 1 and 2 below. They contain an estimated 1–2% disseminated sulphides in random distribution. A total of 10 polished sections with ore minerals have been studied. In boulder 1 chalthallite is associated with a new Tl-sulphide described below as mineral X. Additional ore minerals present are cuprostibite, sphalerite, bornite, galena, antimonian silver and chalcocite-like phases.

The mineral relationships observed suggest that the ore minerals crystallized contemporaneously. In boulder 2 the only Tl-phase present is chalcocite. Ad-

ditional ore minerals identified are galena, sphalerite and seinäjokite. Supergene alteration has resulted in a number of secondary Cu-Sb minerals.

Table 1. Minerals identified or referred to in the present study

|  |   |
|--|---|
| Mineral X  | $Tl_2(Cu,Fe)_6S_5$                        |
| Chalcothallite   | $Tl(K)_2Cu(Fe,Ag)_{6,35}SbS_4$            |
| Rohaite  | $Tl(Pb,K)_2Cu_{8,67}Sb_2S_4$              |
| Thalcosite   | $TlCu_3FeS_4$                             |
| Cuprostibite   | $Cu_2Sb$                                  |
| Gudmundite   | $FeSbS$                                   |
| Seinäjokite  | $FeSb_2$                                  |
| Loellingite  | $FeAs_2$                                  |
| Native silver  | Ag  |
| Allargentum  | (Ag,Sb)                                   |
| Antimonian silver  | $(-Ag_{0,954}Sb_{0,037}Cu_{0,004})$       |
| Chalcosite   | $Cu_{2-x}S$                               |
| Digenite   | $Cu_9S_5$                                 |
| Bornite  | $Cu_5FeS_4$                               |
| Spalerite  | ZnS                                       |
| Galena   | PbS                                       |
| Senarmontite or valentinite                                  | $Sb_2O_3$ (b, Fig.5; b, Fig.6; d, Fig.10) |
| Cuprostibite alteration mineral (c, Fig.5)                   | $PbCu_2(OH)_6nH_2O$                       |
| Cuprostibite alteration mineral (b Fig.7)                    | $(Cu,Fe)Pb_2Sb_{12}(OH)_{24}nH_2O$        |
| Supergene alteration phase after unknown mineral (e, Fig. 6) | $Cu_2Sb_5(OH)_8nH_2O$                     |
| Unidentified Fe-As-mineral (c, Fig.9). Vivianite variety?    | $Fe_3(AsO_4)_2 \cdot H_2O$ .              |
| Ussingite  | $Na_2AlSi_3O_8(OH)$                       |
| Analcime   | $NaAlSi_2O_6 \cdot H_2O$                  |

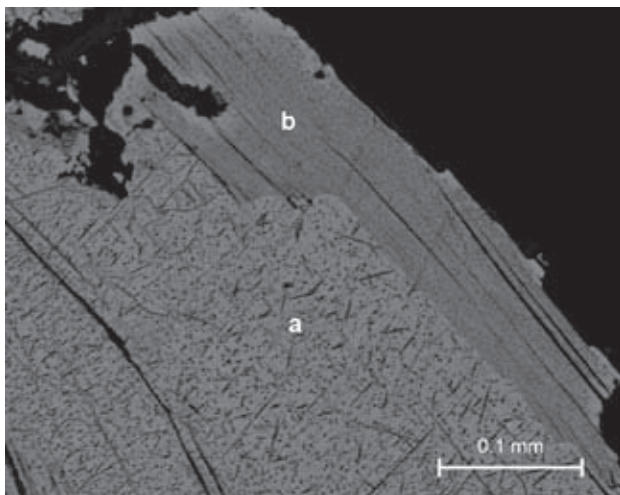


Fig. 1. Grain boundary between chalcothallite (a, composition in Table 3-2) and mineral X (b, Table 2-1). Both minerals show lamellar cleavage. Chalcothallite is dotted by an exsolved phase (Table 3-4) which appears to be oriented after several crystallographic directions in the host. A secondary mineral occurs along cleavage planes in the two Tl-minerals (black lamellae, Table 3-5).

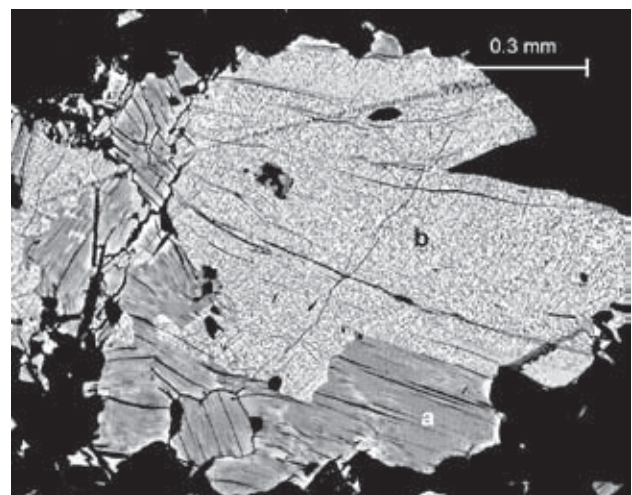


Fig. 2. An aggregate of grains of mineral X (a, Table 2-2) in contact with a large chalcothallite grain (b, Table 4-3) that contains the exsolved phase.

## Microprobe analyses

Electron microprobe analyses were carried out at the Institute of Geography and Geology, University of Copenhagen, using a JEOL 733 superprobe in wavelength dispersive mode, JEOL Pax-11 for instrumental control, and using an on-line ZAF correction program. The excitation voltage was 15 kV and beam current 15 nA. The beam diameter was 1 micron. Wavelengths and standards used were  $\text{CuK}\alpha$ ,  $\text{SbL}\alpha$ ,  $\text{SK}\alpha$  (synthetic

$\text{Cu}_3\text{SbS}_4$ ),  $\text{AsL}\alpha$  (synthetic  $\text{Cu}_3\text{AsS}_4$ ),  $\text{AgL}\alpha$  (Ag),  $\text{ZnK}\alpha$  (synthetic ZnS),  $\text{KK}\alpha$  ( $\text{KAlSi}_3\text{O}_8$ ),  $\text{FeK}\alpha$  ( $\text{Fe}_2\text{O}_3$ ),  $\text{ClK}\alpha$  (sodalite),  $\text{PbL}\alpha$  (PbS),  $\text{SeSeL}\alpha$  (SeS) and  $\text{TlL}\alpha$  ( $\text{TlAsS}_2$ ). The detection limit is estimated to be 0.02 wt.% for all elements. All figures 1–11 are backscattered electron (BSE) images.

Table 2. Microprobe analyses of the new thallium phase – mineral X

|                | 1           | 2           | 3           |
|----------------|-------------|-------------|-------------|
| No of analyses | 5 (Fig. 1)  | 6 (Fig. 2)  | 15          |
| Ag             | 0.09 (11)   | 0.10 (12)   | 0.09 (10)   |
| Cu             | 30.63 (59)  | 29.35 (91)  | 28.82 (57)  |
| Fe             | 10.48 (16)  | 10.50 (30)  | 11.39 (43)  |
| Sb             | 0.12 (9)    | 0.43 (14)   | 0.13 (12)   |
| Tl             | 39.21 (137) | 38.05 (130) | 40.74 (115) |
| K              | 0.97 (42)   | n.a.        | n.a.        |
| S              | 18.46 (31)  | 18.77 (20)  | 19.30 (35)  |
| Total          | 99.96       | 97.2        | 100.34      |
| Molar ratios   |             |             |             |
| Ag             | 0.05        | 0.06        | 0.06        |
| Cu             | 32.93       | 32.39       | 31.06       |
| Fe             | 12.82       | 13.18       | 13.96       |
| Sb             | 0.07        | 0.25        | 0.07        |
| Tl             | 13.11       | 13.06       | 13.65       |
| K              | 1.7         | –           | –           |
| S              | 39.33       | 41.05       | 41.21       |

Average analytical values, wt% (standard deviations in brackets)  
n.a.: not analysed; –: not detected

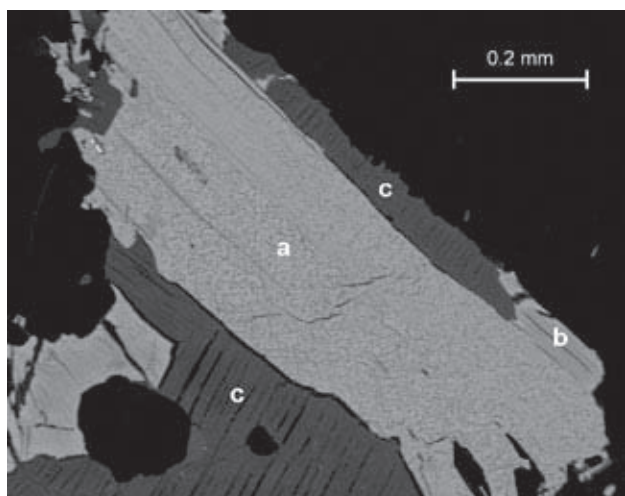


Fig. 3. A relatively large chalcothallite grain with the exsolved unidentified phase (a) in contact with chalcocite (c). On the extreme right a fragment of mineral X (b) lies in contact with chalcothallite and morphologically resembles the associated secondary 'chalcocite'.

## Mineral descriptions

### Mineral X

Due to its softness and fine grain size it was not possible to isolate crystal fragments of this apparently new mineral for single crystal studies. A new mineral name has therefore not been proposed, and it is referred to below as mineral X. In reflected light it is not possible to distinguish mineral X from chalcothallite. In backscattered electron images it is slightly darker than the associated chalcothallite (Figs. 1–3). Mineral X forms lamellar grains with one pronounced cleavage. Cleavage fractures are filled with unidentified secondary products. The mineral occurs either in aggregates with random orientation (bottom part of Fig. 2) or in parallel intergrowths with chalcothallite (Figs. 1–3). It appears to be chemically homogeneous and does not contain inclusions of other minerals. Microprobe analyses carried out on the mineral in two polished sections are listed in Table 2.

Although a crystal structure determination could not be carried out, a model structure for mineral X can be calculated using structural formulae of the known homologues of thalcosite (Kovalenker *et al.*

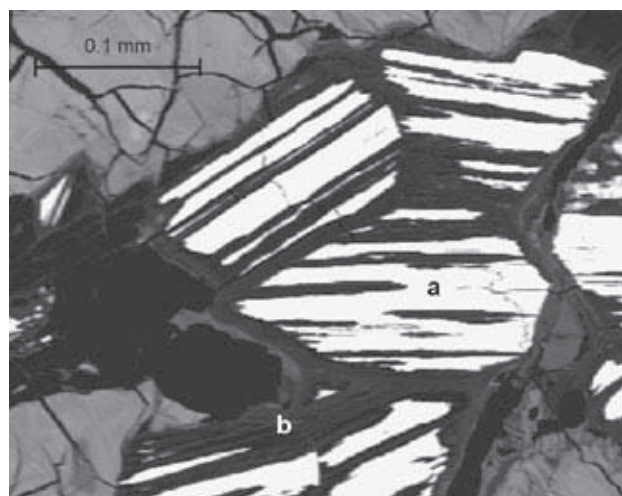


Fig. 4. Aggregate of chalcothallite/mineral X grains (a) partly decomposed to secondary phases (b, Tables 4-1 and 4-2).

1976; Klepp *et al.* 1980; Berger & Eriksson 1990; all summarized in Makovicky 2005). The known homologues are  $N = 1$ , with the model formula  $\text{TlCu}_2\text{S}_2$  with a single-tetrahedron layer;  $N = 2$  with the model formula  $\text{TlCu}_4\text{S}_3$  with a double-tetrahedron layer; and  $N = 3$  with the model formula  $\text{TlCu}_6\text{S}_4$  with a triple-tetrahedron layer. The resulting general formula of the series is  $\text{TlCu}_{2N}\text{S}_{N+1}$  where 'Tl' denotes Tl and K, 'Cu' denotes Cu, Fe and minor Ag, and 'S' stands for S and Se.

There are two ways to calculate the order number  $N$  from the results of chemical analyses:

the ratio of the atomic proportions of the tetrahedral cations, Cu, Fe and Ag to the eight-coordinated cations Tl and K gives:  $N_1 = (\text{Cu} + \text{Fe} + \text{Ag}) / 2(\text{Tl} + \text{K})$ ;

the ratio of anions to the tetrahedral cations:  $(\text{S} + \text{Se}) / (\text{Cu} + \text{Fe} + \text{Ag}) = (N + 1) / 2N$ , simplified hereafter as 'S/Cu', yields:  $N_2 = 1 / (2\text{S} / \text{Cu} - 1) = \text{Cu} / (2\text{S} - \text{Cu})$ . All these expressions are derived from the general formula given above.

These formulae are structure-based and deal with (presumed) structure sites, i.e., they are not concerned with the valency of individual elements. Application of these formulae to the results in Table 2 gives  $N_1 = 1.55$  and  $N_2 = 1.39$  for analysis 1, and  $N_1 = 1.65$  with  $N_2 = 1.21$  for analysis 3. It gives  $N_1 = 1.75$  and  $N_2 = 1.25$  for analysis 2 that contains elevated contents of Sb that are foreign to the structural model applied. The first

two analyses are fairly close to the model with  $N = 1.5$  although the second of these might have somewhat elevated S values, which is reflected in the  $N_2$ -value.

For comparison, thalculusite from the head of the Kangerluarsuk fjord, published by Makovicky *et al.* (1980), has  $N_1 = 1.06$  and  $N_2 = 1.03$ , in agreement with the theoretical value  $N = 1$ .

Parallel to the thalculusite homologous series just described there is a series of Tl-containing channel structures with Cu-S(Se) based channel walls (partitions). They have been summarized in Makovicky (2005, Table 7; 2008, Table 21). Applying the above formulae to this series,  $\text{TlCu}_3\text{Se}_2$  (Berger, 1987) results in  $N_1 = 1.5$  and  $N_2 = 3.0$ ,  $\text{TlCu}_5\text{Se}_3$  (Berger *et al.*, 1990) gives  $N_1 = 2.5$  and  $N_2 = 5$ , and  $\text{TlCu}_7\text{S}_4$  (Berger & Sobott, 1987) yields  $N_1 = 3.5$  and  $N_2 = 7.0$ . All these structures show large systematic discrepancies between the  $N_1$  and  $N_2$  values, very different from our case. Closest to the layer-like results is the structure of  $\text{Rb}_3\text{Cu}_8\text{Se}_6$  (Schils & Bronger, 1979) with  $N_1 = 1.33$  and  $N_2 = 2.0$  since this structure is transitional between a channel and a layer type.

The results indicate that, in full agreement with its appearance, mineral X has a layer structure with, presumably, alternating single- and double-tetrahedron layers, which give the resulting  $N = 1.5$ . When we take a single (Cu,Fe)-Tl sandwich, with a thickness equal to the  $\frac{1}{2}c$  parameter of bukovite (Johan & Kvaček, 1971),

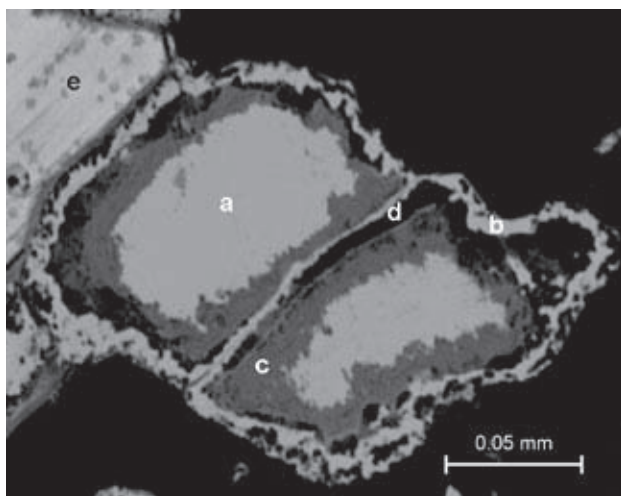


Fig. 5. Two partly decomposed cuprostibite grains (a). The shapes of the original cuprostibite grains are marked by narrow layers of antimony oxide (b, Table 5-2). Remnants of cuprostibite are separated from the antimony oxide by a dark gray layer of a secondary unidentified Cu-Sb-mineral (c, Table 5-1) and unidentified gangue (d). The surrounding gangue mineral (e) is either analcime or ussingite.

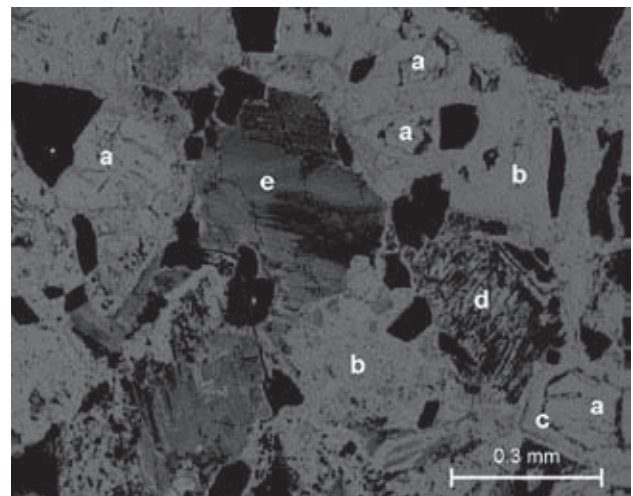


Fig. 6. Extensively decomposed cuprostibite (a). The major part of the alteration area is dominated by antimony oxide (b), very close in composition to that of antimonian oxide in Fig. 5 (Table 5-2). The shape of a cuprostibite crystal is vaguely preserved at the bottom right. The central remnants of the crystal are separated from marginal antimony oxide by a narrow layer of a dark grey Cu-Sb-phase (c). In other places cuprostibite grains are thoroughly penetrated by this phase (d). In the central to left area there is a chemically rather homogeneous mineral (e, Table 5-3) that forms a pseudomorph after an unidentified primary mineral.

i.e. equal to 6.85Å, and a sandwich with a thickness (9.33Å) corresponding to the  $c$  parameter of synthetic  $\text{TlCu}_4\text{Se}_3$  (Klepp *et al.*, 1980), the resulting  $c$  parameter of the 1:1 intergrowth will be 16.18Å. Using the  $c$  (thalcusite)/ $c$ (bukovite) ratio to recalculate selenide to sulfide, the expected  $c$  parameter of mineral X is 15.8Å. The ideal formula for  $N = 1.5$  is  $\text{Tl}_2(\text{Cu,Fe})_6\text{S}_5$ .

The valency of Tl (and K) is  $M^+$  in these structures, and with the divalent anion  $(\text{S,Se})^{2-}$ , the average valency of the tetrahedrally coordinated cations has to be  $v = (2N+1)/2N$  that for  $N = 1.5$  gives  $v = 1.33$ . Valency balance for analyses 1 and 3 in Table 2 gives the average valency of iron as  $\text{Fe}^{2.39+}$  and  $\text{Fe}^{2.68+}$ , respectively, close to  $\text{Fe}^{2.5+}$ .

The ideal formula with  $\text{Fe}^{2.5+}$  is  $\text{Tl}_2\text{Cu}_{4.67}\text{Fe}_{1.33}\text{S}_5$ , i.e. a Cu/Fe ratio of 3.5. The observed ratios are lower, indicating more iron than in the ideal formula, probably because of the deviation of analytical atomic ratios in Table 2 from the ideal value of 15.38 at.% 'Tl', 46.15 at.% 'Cu' and 38.46 at.% S.

## Chalcothallite

In boulder 1 chalcothallite is always characterized by the presence of an exsolved phase that occurs as minute grains evenly distributed throughout the host (Figs. 1–3). A tendency for these to be aligned after several crystallographic directions can sometimes be recognized (Fig. 1). Numerous microprobe analyses were completed on chalcothallite in several polished sections. Selected analyses are listed in Table 3-2 and 3-3. In boulder 2 chalcothallite is homogeneous with no signs of an exsolved phase or inclusions of other minerals. Microprobe analyses of the mineral in two

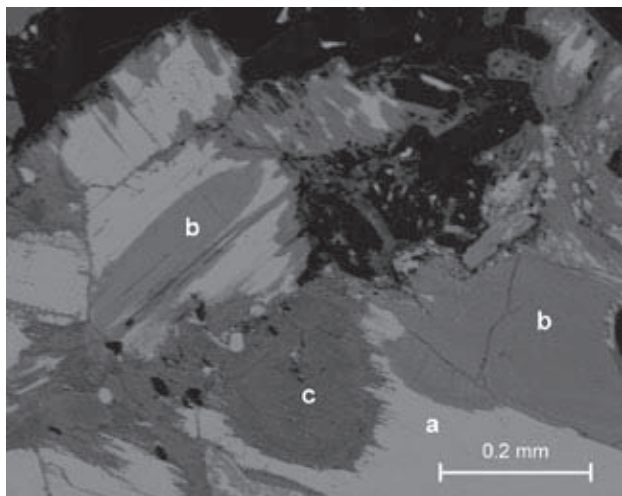


Fig. 7. Cuprostibite grains (a) partly replaced by two secondary Cu-Sb minerals; a dark grey phase (c) (not analyzed, but presumably identical with the dark grey phase in Fig. 5) and a slightly lighter grey phase (b) forming two homogeneous replacement bodies (Table 6-4).

polished sections are listed in Table 3-6 and 3-7.

The fine grain size of the exsolved phase renders quantitative microprobe analysis impossible. A semi-quantitative analysis (Table 3-4) indicates that it is enriched in Ag, Fe, Sb, As, K and S and impoverished in Cu and Tl. Semi-quantitative analyses were also completed on the phase developed along cleavage fractures in chalcothallite grains, such as the grain shown in Fig. 1 (Table 3-5). This phase appears to be a Cu-Sb-Fe-rich oxide/hydroxide, possibly with small amounts of Tl and S. However, due to its fine grain size it cannot be excluded that the low Tl and S-values recorded are due to overlap of the microbeam with the adjacent chalcothallite host.

Supergene alteration of chalcothallite and mineral X has rarely taken place (Fig. 4). Microprobe analyses of the alteration product gave a broad range in compositions, from Cu-rich and Fe-poor (Table 4-1) to Cu-poor and Fe-rich (Table 4-2), with small amounts of Zn and Pb. Nearly all Tl, and most of the Sb, present in the original phase appears to have been removed during the alteration process. The low totals indicate that we are dealing with strongly hydrated products.

## Cuprostibite

Cuprostibite ( $\text{Cu}_2\text{Sb}$ ) has close to ideal composition with only trace amounts of other elements. It is quite common and has been either partly or completely replaced by at least three secondary minerals. In Fig. 5 it is possible to distinguish between two alteration products, a dark phase (c) surrounding remnants of cuprostibite (Table 5-1) with a composition close to  $\text{PbCu}_2(\text{OH})_5 \cdot n\text{H}_2\text{O}$ , and a light grey marginal phase

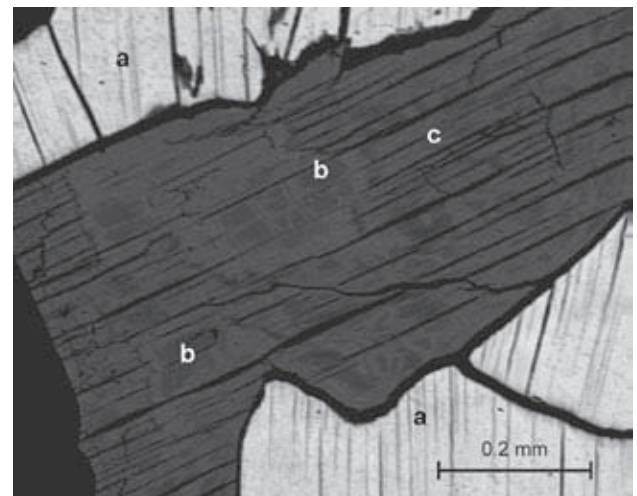


Fig. 8. Mineral X (a) associated with bornite that has almost completely decomposed to a secondary member of the chalcocite group of minerals. Remnants of original bornite (b, Table 6-2) lie embedded in the secondary 'chalcocite' (c, Table 6-1).

(b, Table 5-2), which may be either senarmontite or valentinite ( $\text{Sb}_2\text{O}_3$  with about 1.8 wt% Cu). The shape of the original cuprostibite grains is marked by a thin

rim of this phase. Some areas of strongly decomposed cuprostibite are characterized by relatively large heterogeneous replacement products (Fig. 6) char-

Table 3. Microprobe analyses of chalthallite and associated TI-phases

|                        | 1     | 2          | 3          | 4     | 5           | 6          | 7           |
|------------------------|-------|------------|------------|-------|-------------|------------|-------------|
| No. of analyses        |       | 12         | 7          | 1     | 4           | 9          | 13          |
| Ag                     | 1.32  | 0.50 (15)  | 0.26 (23)  | 1.25  | 0.53 (41)   | 0.03 (7)   | 0.04 (7)    |
| Cu                     | 34.26 | 35.85 (35) | 37.80 (70) | 30.87 | 24.16 (507) | 38.93 (52) | 35.77 (100) |
| Fe                     | 3.88  | 3.63 (16)  | 3.92 (9)   | 8.06  | 7.71 (290)  | 3.81 (6)   | 3.92 (28)   |
| Pb                     | –     | –          | –          | –     | 1.98 (118)  | –          | –           |
| Sb                     | 12.15 | 12.27 (36) | 12.67 (34) | 19.33 | 21.20 (178) | 12.69 (17) | 11.92 (28)  |
| As                     | –     | 0.08 (5)   | 0.09 (7)   | 1.3   | 0.09 (11)   | 0.08 (4)   | 0.13 (5)    |
| Tl                     | 33.94 | 34.95 (70) | 30.01 (53) | 13.37 | 5.16 (376)  | 30.05 (89) | 35.62 (83)  |
| K                      | 0.78  | 0.23 (4)   | 1.58 (10)  | 1.93  | n.a.        | 1.65 (10)  | 0.51 (3)    |
| Te                     | –     | 0.05 (4)   | 0.05 (6)   | 0.17  | 0.04 (4)    | 0.03 (4)   | 0.03 (5)    |
| S                      | 12.54 | 12.78 (24) | 13.02 (15) | 18.74 | 3.74 (111)  | 13.10 (21) | 12.44 (24)  |
| Total                  | 98.87 | 100.34     | 99.4       | 95.02 | 64.48       | 101.37     | 100.38      |
| Molar ratios to S=4.00 |       |            |            |       |             |            |             |
| Ag                     | –     | 0.05       | 0.02       | 0.08  | 0.17        | 0          | 0           |
| Cu                     | 5.51  | 5.5        | 5.86       | 3.33  | 13.04       | 6          | 5.8         |
| Fe                     | 0.71  | 0.65       | 0.69       | 0.99  | 4.73        | 0.67       | 0.72        |
| Pb                     | –     | –          | –          | –     | 0.33        | –          | –           |
| Sb                     | 1.02  | 1.01       | 1.03       | 1.08  | 5.97        | 1.02       | 1.01        |
| As                     | –     | 0.01       | 0.01       | 0.12  | –           | 0.01       | 0.02        |
| Tl                     | 1.7   | 1.72       | 1.45       | 0.45  | 0.86        | 1.49       | 1.8         |
| K                      | –     | 0.06       | 0.4        | 0.34  | –           | 0.41       | 0.13        |
| S                      | 4     | 4          | 4          | 4     | 4           | 4          | 4           |

Average analytical values, wt% (standard deviations in brackets). –: not detected.

Notes. 1: Chalthallite (type specimen) kept at the Geological Museum in Copenhagen. The analysis is reproduced from Makovicky *et al.* (1980). 2 and 3: Composition of chalthallite in two aggregates in boulder 1 (Figs. 1 and 2 respectively). 4: Semi-quantitative analysis of the exsolved phase in chalthallite in Fig. 1. 5: Analyses of fracture-filling in Fig. 1. 6 and 7: Composition of chalthallite in two aggregates from boulder 2.

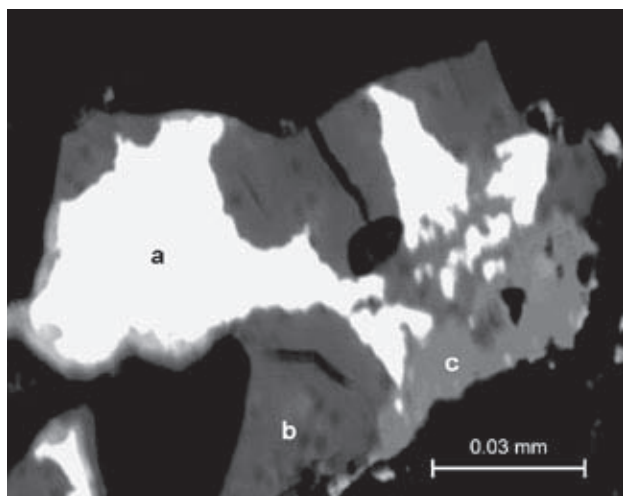


Fig. 9. Galena grain (a) partly replaced by an unidentified member of the chalcosite group of minerals (b, Table 6-4) and an As-rich mineral, possibly a member of the vivianite series (c, Table 6-5).

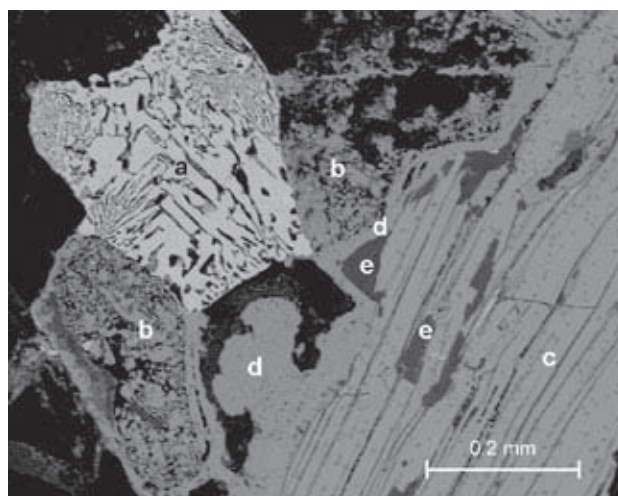


Fig. 10. Exsolution aggregate of antimonian silver (a) enclosed in decomposed cuprostibite grains (b) in contact with chalthallite (c). The outline of the original cuprostibite grains is marked by a narrow layer of grains of antimony oxide (d). A primary phase (e) of the chalcosite group lies interstitial to chalthallite.

acterized by a mixture of, apparently, the same two phases which are nicely separated in Fig. 5. In such material there are, in addition to strongly decomposed cuprostibite, well defined patchy dark grains of an unknown mineral of presumably supergene origin (e, Fig. 6; Table 5-3). It is quite homogeneous with a composition close to  $\text{Cu}_2\text{Sb}_5(\text{OH})_8 \cdot n\text{H}_2\text{O}$ . The identity of the product and of the original mineral remains unknown. Homogeneous replacement patches of a secondary Pb-Sb-oxide/hydroxide into cuprostibite have also been identified (b, Fig. 7, Table 5-4). The simplified empirical composition of this phase may be written as  $(\text{Cu,Fe})\text{Pb}_2\text{Sb}_{12}(\text{OH})_{24} \cdot n\text{H}_2\text{O}$ .

### Bornite-chalcosite group

Relatively coarse bornite crystallized simultaneously with chalcocite and mineral X. Later, presumably supergene alteration of this bornite resulted in the formation of a phase of the chalcosite group with the composition  $\text{Cu}_{1.81}\text{S}$  with small contents of Fe and Sb (Table 6-1). Without X-ray diffraction, unambiguous identification of this phase is not possible due to the small amounts present. In Fig. 8 isolated islands (b) of the original bornite with composition  $\text{Cu}_{1.22}\text{Fe}_{0.29}\text{S}_{1.00}$  (Table 6-2) lie as remnants enclosed in the replacing 'chalcosite'. Areas dominated by this secondary phase are characterized by strong basal cleavage and the cleavage fractures are filled with unidentified products.

Another phase of the chalcosite group with the composition  $\text{Cu}_{2.31}\text{S}$  and with small amounts of Ag, Pb, Sb and Se (Table 6-3) is situated interstitially to chalcocite (Fig. 10) and appears to have crystallized at the same time. Again, identification of this compositionally unusual phase is not possible without X-ray diffraction.

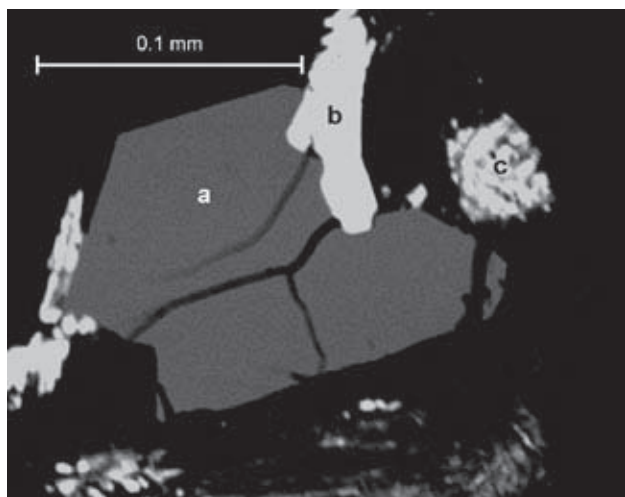


Fig. 11. Crystals of seinäjokite (a) associated with galena (b) and an exsolution aggregate of antimonian silver (c).

### Galena

Galena, in association with both chalcocite-mineral X and cuprostibite, has sometimes been partly replaced by a phase of the chalcosite group with the composition  $\text{Cu}_{1.82}\text{S}$  (b, Fig. 9; Table 6-4). Very rarely this secondary phase is intergrown with an Fe-As-mineral (c, Fig. 9; Table 6-5). The simplified composition of this mineral may be written as  $\text{Fe}_3(\text{AsO}_4)_2 \cdot \text{H}_2\text{O}$  with a minor Cu-content. It is possibly a member of the vivianite series. Galena intergrown with chalcocite in another mineral association has been partly replaced by a chalcosite-like phase with the composition  $\text{Cu}_{2.08}\text{S}$  that contains small amounts of Ag, Pb, Sb and Se (Table 6-6). Small amounts of Cu (0.69(30) wt.%) and Se (0.34(2)wt %) (average of 5 analyses, standard deviation in brackets) was recorded in the galena. The content of Sb is less than 0.04 wt.% and that of Ag is below the detection limit. Galena in two other mineral associations contained smaller amounts of these four elements.

### Sphalerite

Sphalerite is the most common of the ore minerals. It lies isolated in gangue minerals but also occurs as intergrowths with other ore minerals. Small amounts of Cu (0.17(7)wt.%) and Fe (1.25(4) wt.%) (average of 5 analyses) were recorded.

Table 4. Microprobe analyses of decomposition products of chalcocite/mineral X in Fig. 4.

|                 | 1     | 2     |
|-----------------|-------|-------|
| No. of analyses | 2     | 2     |
| Ag              | 0.04  | 0     |
| Cu              | 51.25 | 17.95 |
| Fe              | 7.44  | 30.51 |
| Zn              | 0.33  | 0.87  |
| Pb              | 0.33  | 2.54  |
| Sb              | 0.76  | 1.6   |
| Tl              | 0.01  | 0.35  |
| S               | 4.27  | 1.53  |
| Total           | 64.1  | 55.35 |
| Molar ratios    |       |       |
| Ag              | 0.04  | –     |
| Cu              | 74.57 | 30.82 |
| Fe              | 11.99 | 59.57 |
| Zn              | 0.45  | 1.45  |
| Pb              | 0.33  | 1.33  |
| Sb              | 0.64  | 1.43  |
| Tl              | –     | 0.19  |
| S               | 11.98 | 5.22  |

Average analytical values, wt%  
–: not detected

## Antimonian silver

Rare myrmekite-like aggregates of antimonian silver and an apparently 'decomposed' allargentum phase are associated with both cuprostibite and chalcocite-mineral X (Fig. 10). The antimonian silver has 94.3 wt.% Ag, 4.2 wt.% Sb and 0.26 wt.% Cu ( $\sim\text{Ag}_{0.954}\text{Sb}_{0.037}\text{Cu}_{0.004}$ ), whereas the composition of the intergrown 'decomposed phase' could not be determined due to its small grain size. The chemical composition, texture and optical properties in reflected light of these aggregates suggest that they represent a decomposed high-temperature antimonian silver phase. On cooling this phase dropped into the two-component phase region between antimonian silver and allargentum and thus decomposed into these two phases (see Ag-Sb phase diagram in Somanchi 1966). Alteration of the allargentum variety took place later. Antimonian silver, allargentum and dyscrasite associated with cuprostibite from Ilímaussaq have been described by Karup-Møller (1978a).

## Seinäjokite

Euhedral crystals of seinäjokite ( $\text{FeSb}_2$  with 0.49(4) wt.% Cu) are associated with chalcocite and ga-

lena (Fig. 11). Seinäjokite is known from Ilímaussaq as disseminated grains in lujavrite-MC at Kvanefjeld (Karup-Møller 1978b).

## Discussion

Higher homologues of the thalcosite series ( $\text{TlCu}_{2N-1}\text{S}_{N+1}$ ) are expected to indicate sulphur fugacity in the ore-forming environment that is reduced in comparison to thalcosite-forming solutions. Formation of mineral X therefore parallels the crystallization of chalcocite which is a complex sulphide-antimonide with a rare combination of anions, again made possible by low sulphur fugacity. Further indication of these conditions are cuprostibite, antimonian silver and seinäjokite.

The high content of Fe in mineral X is caused by cation-valency requirements, contrasted by the low Fe-contents of the associated chalcocite, in which the valency requirements are different. The former also contrasts with low Fe-contents in the associated sphalerite, indicating that mineral X and bornite are the principal concentrators of Fe from the solutions generally poor in iron, which also produced the two major gangue minerals ussingite and analcime. Bornite, galena and sphalerite tolerate very varied sulphur

Table 5. Secondary Sb-Cu oxide/hydroxide phases after cuprostibite

|                 | 1                   | 2                                | 3                                | 4                             |
|-----------------|---------------------|----------------------------------|----------------------------------|-------------------------------|
| No. of analyses | 8                   | 3                                | 10                               | 10                            |
| Ag              | 0.11 (10)           | 0.01 (2)                         | 0.06 (1)                         | –                             |
| Cu              | 35.65 (549)         | 1.77 (35)                        | 12.43 (30)                       | 2.24 (17)                     |
| Fe              | 0.14 (2)            | 0.08 (3)                         | 0.03 (3)                         | 0.54 (13)                     |
| Zn              | 0.01 (2)            | –                                | 1.40 (11)                        | –                             |
| Pb              | 0.31 (32)           | –                                | 0.09 (9)                         | 15.28 (104)                   |
| Sb              | 39.25 (430)         | 83.19 (70)                       | 62.59 (92)                       | 54.94 (83)                    |
| Te              | –                   | 0.15 (16)                        | –                                | –                             |
| S               | –                   | 0.08 (7)                         | 0.18 (15)                        | –                             |
| Total           | 75.47               | 85.28                            | 76.78                            | 73.00                         |
| Molar ratios*   |                     |                                  |                                  |                               |
| Ag              | 0.12 <sup>a</sup> – | 0.02 <sup>a</sup> – <sup>b</sup> | 0.07 <sup>a</sup> – <sup>c</sup> | – <sup>a</sup> – <sup>d</sup> |
| Cu              | 63.03 1.74          | 3.90 0.04                        | 26.72 1.90                       | 6.17 0.78                     |
| Fe              | 0.28 0.01           | 0.19 –                           | 0.07 –                           | 1.68 0.21                     |
| Zn              | 0.01 –              | 0.01 –                           | 2.92 0.20                        | – –                           |
| Pb              | 0.17 –              | – –                              | – –                              | 12.95 1.96                    |
| Sb              | 36.22 1.00          | 95.52 1.00                       | 70.22 5.00                       | 79.20 12.00                   |
| Te              | 0.02 –              | 0.36 –                           | – –                              | – –                           |
| S               | 0.15 –              | – –                              | – –                              | – –                           |

Average analytical values, wt% (standard deviations in brackets). –: not detected.

\*Molar ratios: <sup>a</sup> to sum of elements = 100; <sup>b</sup> to Sb = 1.00, <sup>c</sup> to Sb = 5.00, <sup>d</sup> to Sb = 12.00

Notes. 1 and 2: Dark- and light-grey replacement phases after cuprostibite (c and b, Fig. 5). 3: Relatively large mineral grain e, Fig. 6, in matrix of light grey replacement material after cuprostibite (b, Fig. 6). 4: Homogeneous replacement bodies in cuprostibite (b, Fig. 7).



fugacity regimes and do not contradict the above conclusions about low S-fugacity.

The various primary and secondary 'chalcosites' cover a broad compositional range from  $\text{Cu}_{2.32}\text{S}$  to  $\text{Cu}_{1.81}\text{S}$ , and several of them contain small but significant amounts of Fe, Pb and Sb. Without X-ray diffraction data the true identification of these phases is not currently possible.

## Acknowledgements

We are grateful to Mr. T. Weidner who allowed us to work on his collected material. We thank Dr. A. Berger for help with the microprobe analyses and Mr. H. A. Diaz for preparing the polished sections. Dr. H. D. Zimmermann and Dr. T. Balič-Zunič carefully commented on the manuscript. The electron microprobe was financed by the Danish Natural Research Science Council. The research has been partly funded by the Research Council for Nature and Universe (Denmark) under project no. 272-08-227.

## References

- Berger, R. 1987: A phase-analytical study of the Tl-Cu-Se system. *Journal of Solid State Chemistry* 70, 65–70.
- Berger, R. & Ericksson, L. 1990: Crystal structure refinement of monoclinic  $\text{TlCu}_6\text{Se}_4$ . *Journal of Less-Common Metals* 161, 165–173.
- Berger, R. & Sobott, R.J. 1987: Characterization of  $\text{TlCu}_7\text{S}_4$ , a crookesite analogue. *Monatsheft Chemische Wissenschaft* 118, 967–972.
- Berger, R., Ericksson, L. & Meerschaut, A. 1990: The crystal structure of  $\text{TlCu}_5\text{Se}_3$ . *Journal of Solid State Chemistry* 87, 283–288.
- Dobrovol'skaya, M.G. & Nekrasov, I.Ya. 1994: The sulfides of alkali metals and their phase relations in K-Fe-Cu-S system. Abstracts of the 16<sup>th</sup> international General Meeting of the International Mineralogical Association, Pisa, Italy, 99.
- Dobrovol'skaya, M.G., Malov, V.S., Rogova, V.P. & Vyal'sov, L.N. 1984: New find of potassium-bearing thalcosite in charoitic rocks of the Murunskiy pluton. *Doklady Earth Science Section* 267, 171–174.
- Johan, Z. and Kvaček, M. 1971: La bukovite  $\text{Cu}_{3+x}\text{TlFeSe}_{3-x}$ , une nouvelle espèce minérale. *Bulletin Société France Mineralogie* 94, 529–533.
- Karup-Møller, S. 1978a: Primary and secondary ore minerals associated with cuprostibite. *Bulletin Grønlands Geologiske Undersøgelse* 126, 23–47.

Table 6. Primary and secondary Cu-Fe-S phases

|                 | 1                       | 2                       | 3                       | 4                                   | 5              | 6                       |
|-----------------|-------------------------|-------------------------|-------------------------|-------------------------------------|----------------|-------------------------|
| No. of analyses | 7                       | 5                       | 7                       | 11                                  | 6              | 5                       |
| Ag              | 0.10 (10)               | 0.15 (11)               | 0.27 (16)               | 0.36 (32)                           | 0.08 (9)       | 0.24 (13)               |
| Cu              | 77.90 (202)             | 62.13 (131)             | 81.45 (75)              | 71.40 (145)                         | 1.36 (37)      | 76.92 (34)              |
| Fe              | 1.91 (109)              | 13.15 (74)              | 0.02 (3)                | –                                   | 28.83 (57)     | –                       |
| Pb              | –                       | –                       | 1.09 (37)               | 4.94 (120)                          | 0.07 (9)       | 2.22 (36)               |
| Sb              | 0.52 (30)               | 0.19 (21)               | 1.37 (20)               | 3.27 (45)                           | 0.79 (33)      | 3.42 (29)               |
| As              | –                       | –                       | –                       | –                                   | 27.40 (35)     | 0.43 (6)                |
| Se              | –                       | –                       | 0.30 (6)                | 0.73 (6)                            | 0.29 (5)       | 0.43 (6)                |
| S               | 21.74 (21)              | 25.58 (43)              | 17.82 (32)              | 19.84 (52)                          | 0.50 (24)      | 18.63 (21)              |
| Total           | 102.24                  | 101.24                  | 102.32                  | 100.54                              | 59.32          | 101.86                  |
| Molar ratios*   |                         |                         |                         |                                     |                |                         |
| Ag              | 0.05 <sup>a</sup>       | 0.07 <sup>a</sup>       | – <sup>a</sup>          | 0.19 <sup>a</sup> 0.01 <sup>b</sup> | – <sup>a</sup> | 0.12 <sup>a</sup>       |
| Cu              | 63.06 1.81 <sup>b</sup> | 48.62 1.22 <sup>b</sup> | 68.99 2.31 <sup>b</sup> | 62.22 1.81                          | 0.12           | 65.86 2.08 <sup>b</sup> |
| Fe              | 1.75 0.05               | 11.68 0.29              | –                       | –                                   | 2.82           | –                       |
| Pb              | –                       | –                       | 0.28 0.01               | 1.32 0.04                           | –              | 0.58 0.02               |
| Sb              | 0.22                    | 0.08                    | 0.60 0.02               | 1.49 0.04                           | 0.04           | 1.53 0.05               |
| As              | –                       | –                       | –                       | –                                   | 2              | –                       |
| Se              | 0.05                    | –                       | 0.21 0.01               | 0.51 0.01                           | 0.02           | 0.30 0.01               |
| S               | 34.87 1.00              | 39.55 1.00              | 29.92 1.00              | 34.26 1.00                          | 0.09           | 31.61 1.00              |

Average analytical values, wt% (standard deviations in brackets). –: not detected.

\* Molar ratios: <sup>a</sup> to sum of elements = 100.0; <sup>b</sup> to S = 1.00

Notes. 1: Chalcosite group phase (c, grey, Fig. 8) partly replacing 2; 2: Bornite (b, dark grey, Fig. 8); 3: Primary Cu-S phase interstitial to chalcocite; 4: Secondary chalcosite group phase; 5: As-rich mineral of the vivianite group of minerals partly replacing galena (b, c and a respectively in Fig. 9); 6: Secondary chalcosite group phase partly replacing galena enclosed in chalcocite.

- Karup-Møller, S. 1978b: The ore minerals of the Ilímaussaq intrusion: their mode of occurrence and their conditions of formation. *Bulletin Grønlands Geologiske Undersøgelse* 127, 51 pp.
- Karup-Møller, S. & Makovicky, E. 2001: Thalcusite from Nakkalaqaq, the Ilímuassaq alkaline complex, South Greenland. *Geology of Greenland Survey Bulletin* 190, 127–130.
- Klepp, K.O., Boller, H. & Völlenkne, H. 1980: Neue Verbindungen mit  $\text{KCu}_4\text{S}_3$ , Struktur. *Monatshefte für Chemie* 111, 727–733.
- Kovalenker, V.A., Laputina, I.P., Yevstigneyeva, T.L. & Izoitko, V.M. 1976: Thalcusite  $\text{Cu}_{3-x}\text{Tl}_2\text{Fe}_{1-x}\text{S}_4$ ; a new sulfide of thallium from copper-nickel ores of the Talnakh Deposit. *Zapiski Vsesoyuznogo Mineralogicheskogo Obshchestva* 105(2), 202–206 (in Russian).
- Kovalenker, V.A., Laputina, I.P., Semenov, E.I. & Yevstigneyeva, T.L. 1978: Potassium-bearing thalcusite from the Ilímaussaq pluton and new data on chalthallite. *Doklady Akademii Nauk SSSR* 239, 1203–1206 (in Russian). (Translation: *Doklady Earth Science Sections* 239, 159–162).
- Makovicky, E. 2005: Micro and mesoporous sulfide and selenide structures. *Reviews in Mineralogy and Geochemistry* 57, 403–434.
- Makovicky, E. 2008: Crystal structures of sulfides and other chalcogenides. *Reviews in Mineralogy and Geochemistry* 61, 7–125.
- Makovicky, E., Johan, Z. & Karup-Møller, S. 1980: New data on bukovite, thalcusite, chalthallite and rohaite. *Neues Jahrbuch für Mineralogie Abhandlungen* 138, 122–146.
- Mandarino, J.A. & Anderson, V. 1989: *Monteregian Treasures, the Minerals of Mont Saint-Hilaire, Quebec* 281 pp. Cambridge: Cambridge University Press.
- Mookherjee, A., Mozgova, N.N., Golovanova, T.I. & Mishra, B. 1984: Rare minerals from Rajapura-Dariba, Rajasthan, India VI: Thalcusite, its geochemical significance. *Neues Jahrbuch für Mineralogie Monatshefte* 10, 444–454.
- Schils, H. & Bronger, W. 1979: Ternäre Selenide des Kupfers. *Zeitschrift Anorganische Allgemeine Chemie* 456, 187–193.
- Semenov, E.I., Sørensen, H., Bessmertnaja, M.S. & Novorossova, L.E. 1967: Chalthallite – a new sulphide of copper and thallium from the Ilímaussaq alkaline intrusion, South Greenland. *Bulletin Grønlands Geologiske Undersøgelse* 68, 13–26 (also *Meddelelser om Grønland* 181(5)).
- Somanchi, S. 1966: Subsolidus phase relations in the system Ag–Sb. *Canadian Journal of Earth Sciences* 3, 211–272.